Ultrasound in Med. & Biol., Vol. 28, No. 3, pp. 349–358, 2002

0301-5629/02/$–see front matter

PII: S0301-5629(01)00516-6

● *Original Contribution*

TIME-INTENSITY-BASED VOLUMETRIC FLOW MEASUREMENTS: AN *IN VITRO* STUDY

PAI-CHI LI, CHIH-KUANG YEH and SHENG-WUEI WANG
Department of Electrical Engineering, National Taiwan University, Taipei, Taiwan

(*Received* 2 *July* 2001; *in final form* 10 *December* 2001)

Abstract—Ultrasonic contrast agents have been used to assist blood flow measurements. Several contrast-specific flow measurement techniques have been proposed during the last few years. Among them, a method based on relative enhancement of the backscattered signal as a function of time is of particular interest. This method is also known as the time-intensity method. The method is based on the indicator-dilution theory, and the time-intensity curve is used to derive blood flow-related parameters such as the flow rate and the blood mixing volume. Previous *in vitro* studies done by other research groups were mainly based on a perfusion model or an artery model. Results showed that several parameters derived from the time-intensity curve had a good correlation with the flow rate under certain conditions. However, the studies did not focus on factors such as mixing volume, mixing chamber configuration and different types of mixing chamber. In this paper, dependence of the time-intensity curve is further studied. Specifically, two types of blood-mixing chambers were constructed. One was a spherical compartment phantom with two different sizes (260 and 580 mL) and different inflow/outflow configurations. The other was a perfusion phantom consisting of dialysis cartridges with the volume ranging from 114 to 351 mL. The time intensities were also measured at both the input and the output of the mixing chamber. A commercial agent (Levovist®) and a self-made, albumin-based agent were used and the wash-out time constant and the mean transit time were derived for flow rates ranging from 500 to 1300 mL/min. For the perfusion phantom, results showed that the parameters had a good correlation with both the flow rate and the mixing volume. Results from the compartment phantom, on the other hand, indicated that the inflow/outflow configuration and the mixing size significantly affected the derived time constants. Potential applications of new volumetric flow estimation techniques based on both input and output intensities were also discussed. (E-mail: paichi@cc.ee.ntu.edu.tw)

Key Words: **Ultrasonic contrast agent, Time-intensity curve, Volumetric flow measurement.**

INTRODUCTION

Ultrasound (US) has become increasingly popular in medical diagnosis. Among the major clinical applications, blood flow measurement is of particular importance. Conventionally, the Doppler effect is used to acquire blood flow information. In this case, blood velocity is measured by detecting the frequency change of echoes backscattered from the moving blood. Despite its wide clinical acceptance, the utility of Doppler-based methods in quantitative volumetric flow estimation has been limited (Burns and Jaffe 1985). One of the limitations is the difficulty in obtaining the beam-to-flow angle (Li et al. 2000, 2001). Variations of the area of a vessel over a heart cycle and flow turbulence also make quantitative flow measurements practically difficult.

In addition to conventional Doppler techniques, new techniques for ultrasonic blood flow measurements have also been continuously developed. The use of ultrasonic contrast agents is a good example (Frinking et al. 2000; Goldberg 2000). Many contrast agents are air-filled microbubbles that dissolve poorly in the blood. The bubbles are small enough so that they can reach the left ventricle of the heart and avoid rapid disappearance. Contrast-specific imaging techniques have also been proposed and they can be categorized into three groups. The first group is based on the enhanced echo signal at the fundamental frequency. Ultrasonic contrast agents improve blood flow detection and offer possibilities of visualizing perfusion conditions (Navin and Reinhard 1993). The second group is based on the nonlinear response due to oscillation of the contrast agent. Examples

Address correspondence to: Pai-Chi Li, Department of Electrical Engineering, National Taiwan University, No.1, Sec. 4, Roosevelt Road, Taipei 106 Taiwan. E-mail: paichi@cc.ee.ntu.edu.tw

are harmonic imaging and subharmonic imaging (Frinking et al. 2000). The third group of contrast-specific techniques is based on dilution and destruction of microbubbles in the blood pool (Claassen et al. 2001; Chen et al. 1998; Hindle and Perkins 1994; Schwarz et al. 1993, 1996; Ugolini et al. 2000; Wilkening et al. 1999, 2000; Wilson et al. 1993). Note that the indicator-dilution theory has already been used in other imaging modalities (Axel 1980; Blomley et al. 1995). With the development of microbubble-based ultrasonic contrast agents, it is possible to institute a noninvasive technique to measure hemodynamic parameters based on dilution of microbubbles.

The indicator-dilution theory is based on the law of mass conservation. After a dose of indicators is injected into the blood, the concentration of the agent is monitored as a function of time. The signal-enhancement effect of the contrast agent can be used to monitor concentration of the agent and to make quantitative indicator-dilution–style measurements. Such a method is also known as the time-intensity method. In general, after injection, the microbubbles are mixed in a few compartments in the circulatory system. Each of these compartments can be treated as a simple mixing chamber. The mixing process inside the chamber can be described by a simple mathematical model and the response from each chamber can be characterized by a transfer function. Thus, by considering concentration of the indicator entering the mixing chamber as the input function, the output function defined as the concentration leaving the chamber is simply the convolution of the input function and the transfer function (Chen et al. 1998). With multiple mixing chambers in cascade connection, the same procedure can be repeated. The flow rate and the volume of the mixing chamber can then be derived if the transfer function of a particular mixing chamber can be estimated.

Several recent studies have focused on contrast-based flow quantification. In particular, effects of the flow rate on the measured time intensities have been extensively studied (Claassen et al. 2001; Chen et al. 1998; Hindle and Perkins 1994; Schwarz et al. 1993a, 1993b, 1996; Ugolini et al. 2000; Wilkening et al. 1999, 2000; Wilson et al. 1993). In the study of Ugolini et al. (2000), absolute and relative flow quantification was performed using harmonic power Doppler imaging. A good correlation between the absolute flow and several parameters derived from the time-intensity curve was found in a perfusion model. The perfusion model was composed of dialysis cartridges and the derived parameters included onset time, time-to-maximal enhancement, peak intensity and maximal ascending slope. The correlation for a tube model was also investigated. It was found that, for absolute flow quantification, the correlation for the tube model was lower than that for the perfusion model. Nonetheless, the correlation in both models was improved when only relative flow quantification was concerned. Quantification of flow rates was also investigated using harmonic grey-scale imaging (Claassen et al. 2001). Again, a dialysis cartridge was used to produce a capillary flow model. Peak signal intensity, area under the curve and mean transit time were the main parameters of interest. It was found that the indicator-dilution theory is not applicable for perfusion analysis, possibly due to the effect of bubble saturation.

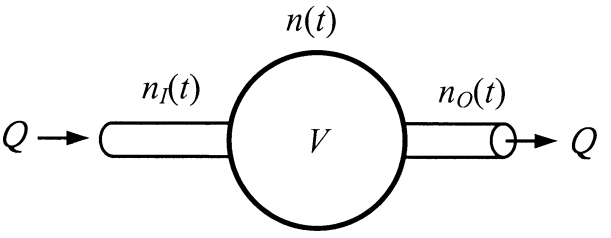

Fig. 1. A schematic diagram of the mixing chamber model.

In addition to the perfusion model with a fixed volume, absolute and relative volumetric flow rates were also studied in an arterial model with two different sizes (Schwarz et al. 1993a). Three ultrasonic time-intensity methods (RF, video and Doppler) were tested. It was shown that the mixing volume affected results of absolute volumetric flow rate measurements. Relative measurements, on the other hand, were independent of the mixing volume. Finally, an *in vivo* study on quantitating myocardial perfusion with a dog model was also performed (Wilson et al. 1993). It was found that the time-intensity techniques may be feasible with intracoronary injections, but there was no appreciable intensity change with IV injections.

In this study, correlation between the time-intensity curve and various experimental conditions was further determined. Specifically, the time-intensity curve was measured with different sizes of two types of blood-mixing phantoms. One is a compartment phantom made of a hollow sphere and the other is a perfusion phantom consisting of a maximum number of four dialysis cartridges. Also, the influence of the inflow/outflow configuration for the compartment model was investigated. This paper concludes with a discussion of potential new flow quantification techniques based on both input and output intensities.

BASIC PRINCIPLES OF THE TIME-INTENSITY TECHNIQUE

Consider the simple model depicted in Fig. 1. Blood flow of rate Q enters and leaves a blood-mixing chamber

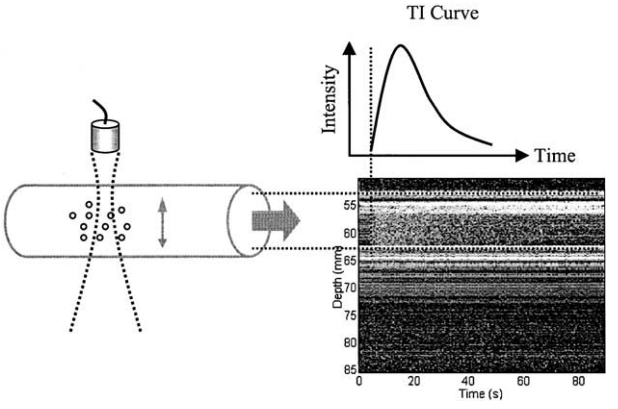

Fig. 2. Illustration of generation of the time-intensity curve.

of volume *V via* a single input vessel and a single output vessel. As the contrast agent is entering the chamber, the concentration as a function of time (*i.e.*, the input function) is defined as $n_I(t)$. According to the indicator-dilution theory, the concentration of the contrast agent at the output end (*i.e.*, the output function $n_o(t)$) is given by:

$$n_o(t) = n_I(t) \otimes h(t), \tag{1}$$

where $\otimes$ stands for convolution and $h(t)$ is the transfer function of the mixing chamber. Note that the concentration is not directly measured in practice. Instead, the backscattered acoustic intensity is used to represent the concentration of the microbubbles (Schwarz et al. 1993b). Such an approximation may not be valid when the bubble concentration is high (Wilson et al. 1993; Claassen et al. 2001). In this study, the concentration was empirically determined so that the linear relationship between the backscattered intensity and the concentration was valid while maintaining a sufficient signal-to-noise ratio (SNR). Figure 2 is a schematic diagram of generation of the time-intensity curve. Assuming a transducer focuses a sound beam in a vessel, as shown in the left panel, the lower right panel shows a corresponding M-mode image with the horizontal axis denoting time and the vertical axis representing depth. At each time instance, intensities of the backscattered signals within the vessel are averaged and the average value becomes a point in the time-intensity curve shown in the upper right panel. This process continues at all times until a complete time-intensity curve is generated. Note that the reverberation signals shown in the M-mode image can be easily removed by subtracting the baseline from the raw time-intensity data.

The transfer function $h(t)$ contains characteristics of the blood-mixing chamber (Chen et al. 1998). The simplest form of the transfer function can be described by a single time constant. The time constant τ can be considered as the system's transit time and is defined as the ratio of the mixing chamber volume to the volume flow rate (*i.e.*, $\tau = V/Q$. Specifically, the transfer function is given by:

$$h(t) = \begin{cases} 0 & t < 0 \\ \dfrac{I}{\tau} e^{-t/\tau} & t > 0 \end{cases} \tag{2}$$

It is assumed that the microbubbles are completely mixed with blood inside the mixing chamber. This assumption may not be true in practice and may affect results of time-constant estimation. The time constant τ is also known as the wash-out time constant (*i.e.*, $1/\tau$ is the wash-out rate).

In addition to τ, the mean transit time (MTT) defined in eqn (3) can also be employed:

$$MTT = \frac{\int_0^\infty t \times n_o(t)dt}{\int_0^\infty n_o(t)dt}. \tag{3}$$

If duration of the input function $n_I(t)$ is significantly smaller than τ, the input can be approximated as an impulse function and the output $n_o(t)$ approximates the impulse response $h(t)$. In this case, in can be easily shown that MTT = τ. Generally, the input function may have an arbitrary form because it can be the output function of a previous mixing chamber. In this case, both the input and the output need to be measured and deconvolution techniques can be applied to find the transfer function. In the following section, we will focus on the two parameters MTT and τ and assume that the duration of the bolus injection is sufficiently small that the output function approximates the transfer function of the mixing chamber. Also, note that the transfer function described in eqn (2) may not be applicable to all types of mixing chambers. As will be shown in the next section, the transfer function of the perfusion phantom has different characteristics and will be modeled by a different function.

Methods and Materials

Spherical compartment phantoms (Ostrander et al. 1990) and perfusion phantoms (Hindle and Perkins 1994; Claassen et al. 2001) were constructed. The spherical compartment phantom was made of an acrylic hollow sphere. The perfusion phantom, on the other hand, consisted of four renal dialysis cartridges (C-12, Terumo

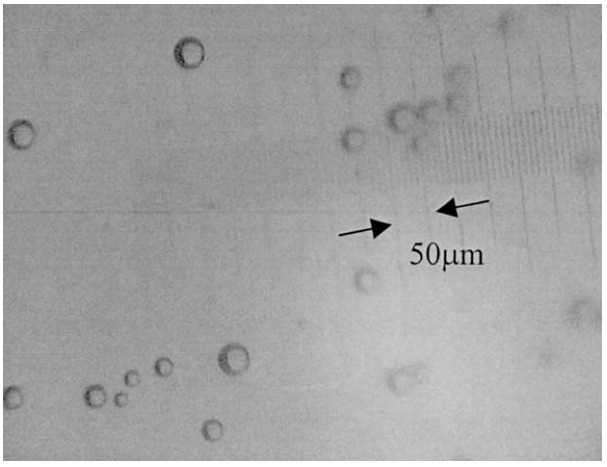

Fig. 3. Photograph of the self-made albumin-based contrast agent. The distance between two arrows corresponds to 50 μm.

Co., Tokyo, Japan) placed in parallel. Each cartridge consisted of 8600 hydrophilic capillaries and each capillary had a mean diameter of 200 μm and a length of 235 mm, making a total capillary volume of 79 mL.

Both a self-made albumin-based contrast agent and Levovist® were used in the study. The self-made contrast agent was made from albumin using the hand agitation technique (Navin and Reinhard 1993). Two 10-mL plastic syringes (Terumo Co.) were connected to a three-way stopcock (NIPRO Med Ltd., Osaka, Japan) and a needle was connected to the third end. Four ml of water, 1 mL of 20% human albumin solution (Octapharma AG, Vienna, Austria) and 0.5 mL of air were mixed at one of the syringes. The two syringes were then pushed in turn, with the valve of the three-way stopcock closed at the needle site. After several pushings, a layer of foam was formed on the top of the solution. The fluid below the foam layer was used as the US contrast agent. The size of the self-made microbubbles was estimated using an optic microscope (EMZ-TR, Meui Tech. Co., Tokyo, Japan). The diameter ranged from 20 μm to 50 μm. A picture of the albumin-based contrast agent from the microscope is shown in Fig. 3.

The experimental system consisted of two data-acquisition subsystems. One was to acquire acoustic data from the input vessel of the mixing chamber and the other was for the output vessel. The input subsystem consisted of a pulser/receiver (Panametrics 5800, Waltham, MA), a 12-bit, 20 Msamples/s A/D (HP E1425A) and a 12-bit, 40 Msamples/s arbitrary function generator (HP E1445A). The equipment was controlled by a personal computer *via* VEE software (HP E1425A, Palo Alto, CA). The output subsystem had a similar configuration. It included a pulser/receiver (Panametrics 5072), a data-acquisition system with a 12-bit, 80

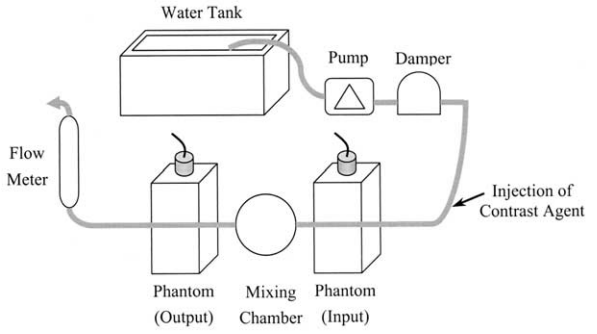

Fig. 4. Experimental setup with the spherical compartment phantom.

Msamples/s arbitrary function generator (CompuGen 1100, Gage, Montreal, Canada) and a 12-bit, 100 Msamples/s A/D (CompuScope 12100, Gage, Montreal, Canada). The equipment was controlled by a personal computer *via* LabVIEW (National Instruments, Austin, TX). The arbitrary function generator of the input subsystem was also used for synchronization between the input and the output subsystems. After the returning echoes were received and amplified by both subsystems, the signals were then sampled and stored for off-line signal processing. The intensity data were sampled at a rate of 1 Hz. Data analysis and graphic display were done on a personal computer using MATLAB (MathWorks, Natick, MA). Two identical transducers (Panametrics V380) were used in the two subsystems. Both transducers had a center frequency at 3.5 MHz and a fixed focus at 70 mm. A pump (Cole-Parmer L/S-18, 77201-60, Vernon Hills, IL), silicone peroxide-cured tubing with an 8-mm diameter (Cole-Parmer L/S-18), a shielded flowmeter (Gilmont Instruments GF-2560, Barrington, IL) and a damper (Cole-Parmer LC-07596-20) comprised of the flow system. Note that the damper was used to eliminate flow pulsation and to create a laminar flow. Schematic diagrams of the data acquisition system with the spherical compartment phantom and the perfusion phantom are shown in Figs. 4 and 5, respectively.

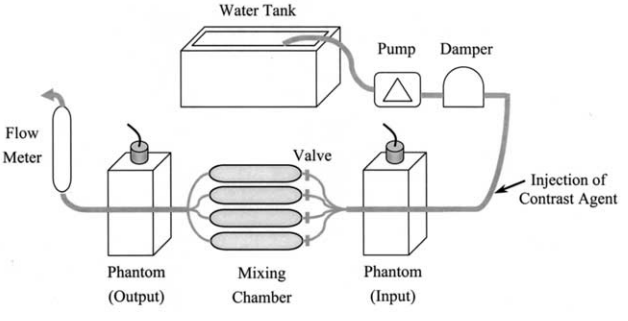

Fig. 5. Experimental setup with the perfusion phantom.

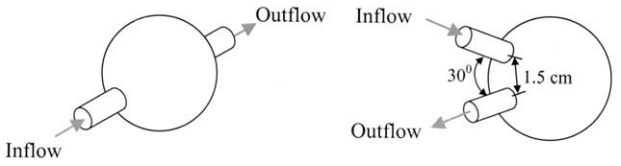

Fig. 6. Two different compartment phantoms. Left: same inflow/output direction. Right: opposite inflow/outflow directions.

EXPERIMENTAL RESULTS

The first set of experiments was performed to study effects of flow directions on the measured time-intensity curves. Two spherical compartment phantoms were constructed, as shown in Fig. 6. The phantom on the left had the inflow and the outflow along the same direction (*i.e.*, the input/output vessels were placed on opposite sides). The phantom on the right had the inflow and the outflow along opposite directions (*i.e.*, the two vessels were placed on the same side). The estimated time constants associated with the two phantoms as a function of the flow rate are shown in Fig. 7a and b, respectively. The time constants were derived from least-square fitted exponential time-intensity curves based on the output measurements. In both figures, the MTTs are represented by the dashed lines and the τs are represented by the dotted lines. For all data, the mean value of five independent measurements is shown, with the error bar indicating $\pm$ 1 SD. The theoretical values shown by the solid lines were obtained by dividing the total volume of the sphere (*i.e.*, *V*) by the volume flow rate measured by the flowmeter (*i.e.*, *Q*). The total volume of the sphere in this case was 260 mL and the flow rate ranged from 500 mL/min to 1300 mL/min. It is shown that the MTT values in Fig. 7b (*i.e.*, opposite inflow/outflow directions) are in good agreement with the theory. On the other hand, the τs in Fig. 7b were significantly lower than the theoretical values, although a general inverse trend was present between the time constant and the flow rate. Both time constants shown in Fig. 7a, on the other hand, did not follow the inverse relationship with the flow rate.

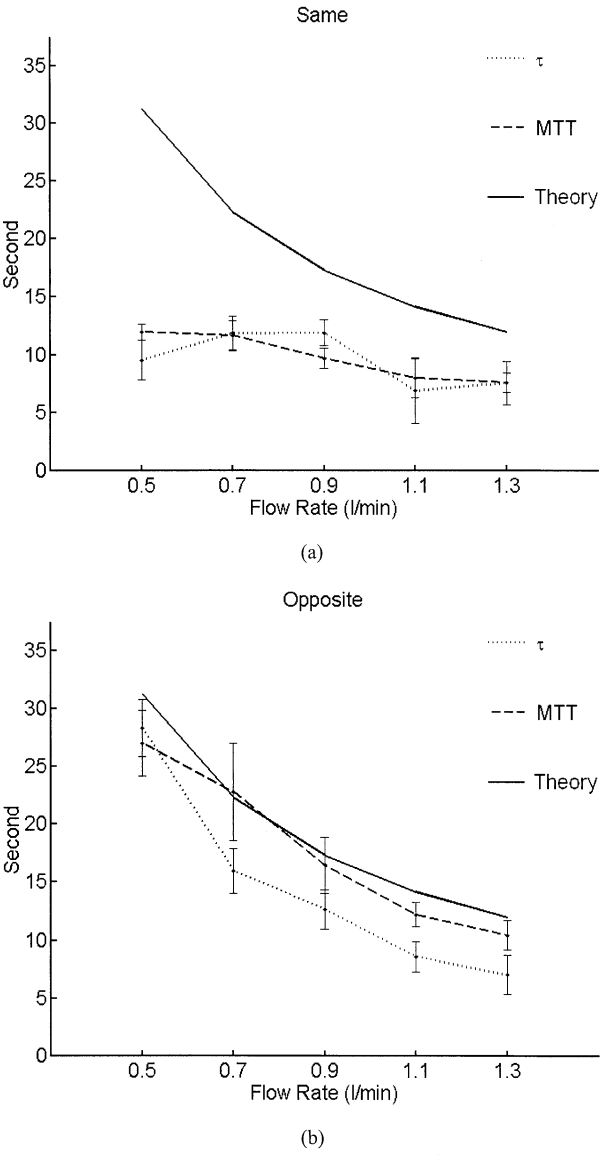

Fig. 7. Time constants measured using the spherical compartment phantom (260 mL). (a) Same inflow/output direction; (b) opposite inflow/outflow directions.

Figure 8 shows the corresponding time-intensity curves, to offer possible explanation for the results depicted in Fig. 7. Figure 8a shows the input (left) and output (right) intensities as a function time for the mixing chamber shown on the left of Fig. 6 (*i.e.*, same flow direction). Figure 8b shows results for the mixing chamber shown on the right of Fig. 6 (*i.e.*, opposite flow directions). The volumetric flow rate in this case is 500 mL/min; thus, making the theoretical value of the time constant 31.2 s. As shown in this figure, duration of both input functions is significantly smaller than the theoretical time constant. Thus, the input can be approximated by an impulse function and the output approximately represents the transfer function of the mixing chamber.

Although the two input functions are similar to each other, the two output intensity curves shown in Fig. 8 are significantly different. As shown in Fig. 8a, the output intensity curve consists of a peak very similar to the input function, followed by a region that resembles a typical exponential wash-out curve. This may result from the fact that many microbubbles pass directly through the mixing chamber without being completely diluted, due to the particular inflow/outflow configuration. It is also consistent with the fact that the estimated time constants

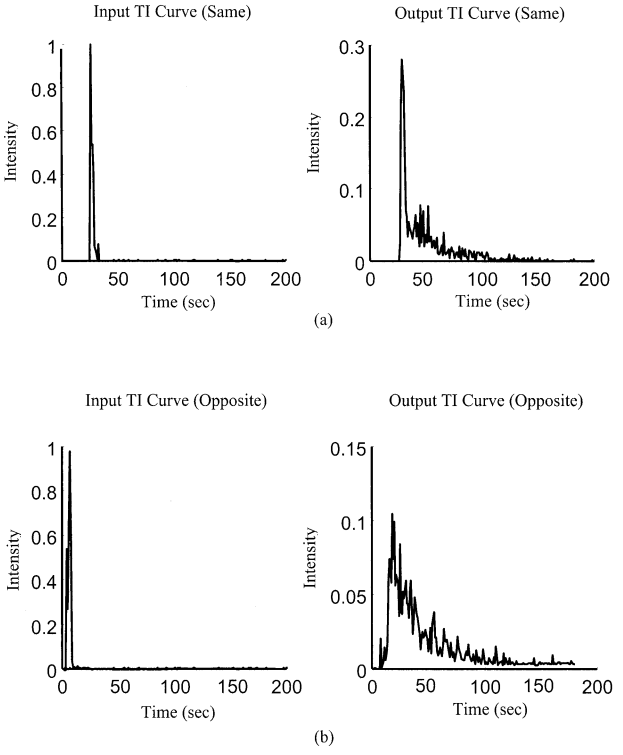

Fig. 8. Measured time-intensity curves. (a) Left: input/same direction; right: output/same direction; (b) left: input/opposite directions, right: output/opposite directions.

are smaller than the theoretical values (*i.e.*, a smaller effective mixing volume). When the inflow and the outflow have opposite directions, on the other hand, mixing is more complete; the entire curve can be viewed as a typical exponential wash-out curve. In this case, the MTT curve is in good agreement with the theory. The wash-out time constant τ is smaller than the MTT in both cases, possibly due to the nonnegligible measurement noise. In other words, the MTT is a more robust measure of the time constant in this case.

The same set of experiments with opposite flow directions was also performed using Levovist® and results are shown in Fig. 9. Again, the MTT curve is in good agreement with the theory and the τ curve is lower than the MTT curve. The τ curve of Levovist® is also lower than that of the self-made albumin-based contrast agent shown in Fig. 7a. Again, MTT is less affected by the differences in measurement conditions.

Another set of experiments was performed with a larger spherical compartment phantom. The volume was 580 mL and opposite inflow/outflow directions were used. The estimated time constants are shown in Fig. 10. Again, MTTs are larger than the τs. Unlike the results from a smaller chamber, however, the MTT curve is lower than the theoretical curve in this case. This indicates that the effective mixing volume may be smaller than the physical volume of the chamber. Nonetheless, the effective mixing volume is still larger than the volume used in Fig. 7 (*i.e.*, larger than 260 mL) and the inverse trend between the flow rate and the MTT is still present.

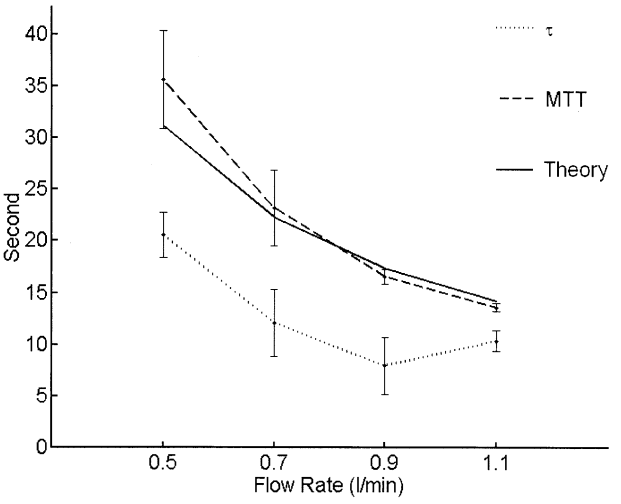

Fig. 9. Time constants measured with Levovist®.

Finally, experiments were performed with the perfusion phantom. There were four cartridges in total and each cartridge was independently connected or disconnected by controlling valves at the ends of the cartridges. The number of connected cartridges determined the overall volume of the mixing chamber. Because the volume of a single cartridge was 79 mL and the volume in the connecting tubes was 35 mL, the total volume of

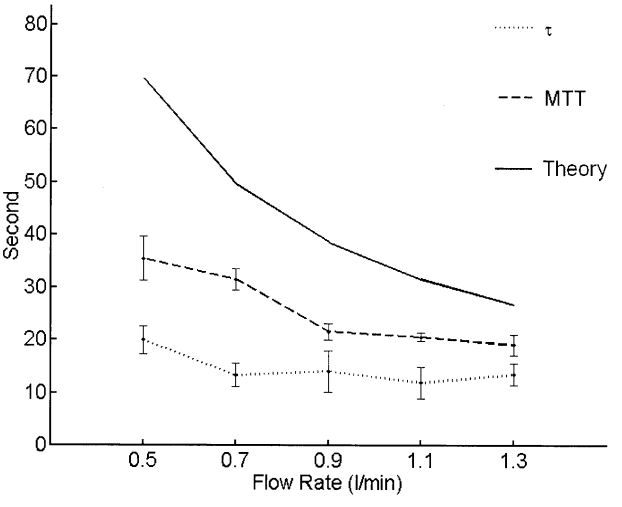

Fig. 10. Time constants measured with a larger compartment phantom (580 mL).

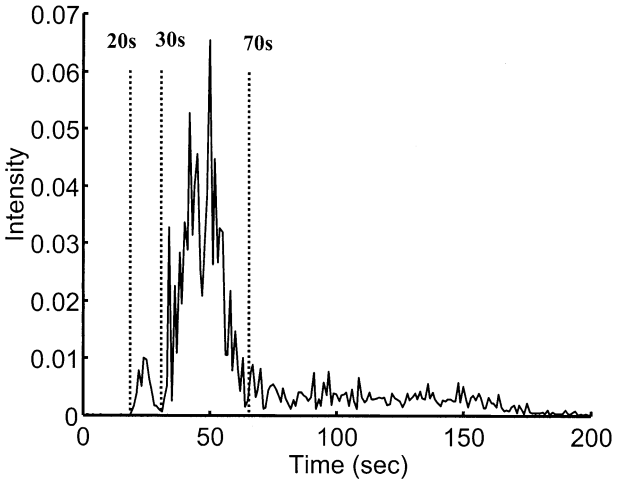

Fig. 11. A typical time-intensity curve with the perfusion phantom.

the perfusion phantom varied from 114 (*i.e.*, 79 + 35) to 351 mL (*i.e.*, 79 × 4 + 35). Figure 11 shows a typical output time-intensity curve measured from a perfusion phantom. The curve can be divided into three regions. The first region is between 20 s and 30 s and it corresponds to the case where microbubbles directly pass through the cartridges without much dilution. This is similar to the output curve shown in Fig. 8a. The second region is from 30 s to 70 s and it relates to a more complete mixing and dilution of the microbubbles. Note that characteristics of the time-intensity curve in this region differ from those associated with the compartment phantom shown in Fig. 8b. Specifically, the backscattered intensity does not increase as rapidly in Fig. 11 as in Fig. 8b. Thus, the time-intensity data were fitted to a gamma function instead of to an exponential function. A gamma function has the following form:

$$g(t) = \alpha(t - t_0)^{\gamma} e^{-\beta(t-t_0)}, \qquad (4)$$

where α and β are scaling factors and γ represents the skewness.

The third region is after 70 s and it corresponds to an elevated baseline. In this region, some microbubbles may have been trapped in the dialysis cartridges and they moved much slower than the overall blood velocity. The estimated time constants from the second region with γ-curve-fitting are shown in Fig. 12. In both panels, ×, o, + and * represent estimated mean time constants of 10 independent measurements, with the error bar representing ± 1 SD for flow rates of 500, 700, 900 and 1100 mL/min, respectively. The τs are shown in the top (Fig. 12a) and the MTTs are shown in the bottom (Fig. 12b). The horizontal axis represents the number of dialysis

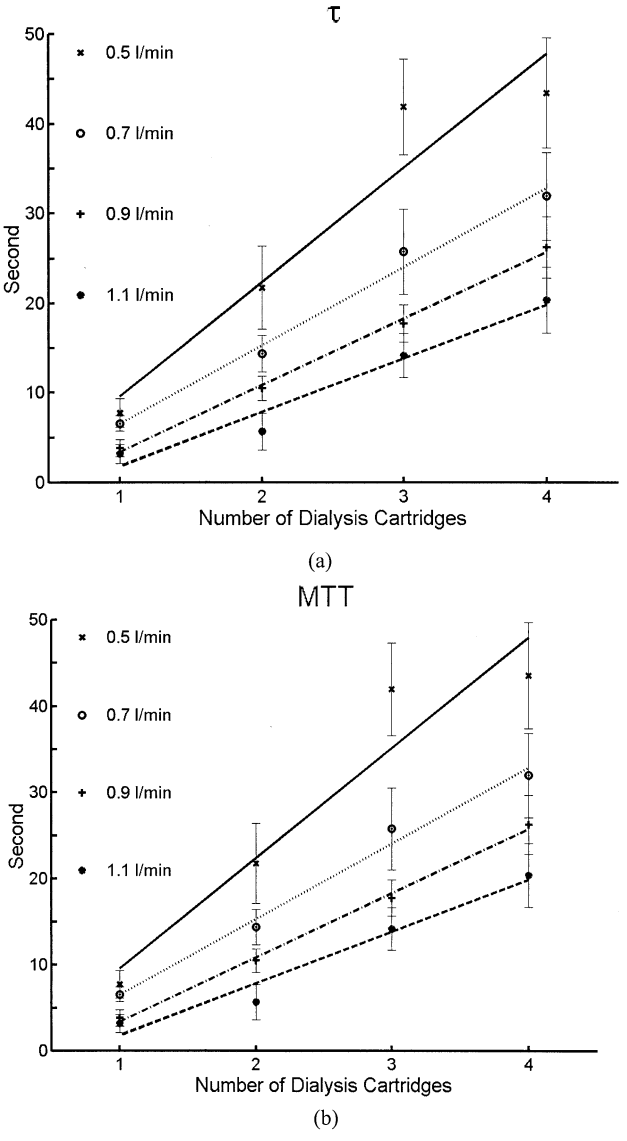

Fig. 12. Time constants measured with the perfusion phantom. The horizontal axis is the number of connected dialysis cartridges. (a) τ; (b) MTT.

cartridges connected and it is approximately linearly proportional to the total volume. The least-square-fitted lines are also shown. In general, the time constants are linearly proportional to the total volume of the mixing chamber. For a fixed number of connected dialysis cartridges, the time constants also decreased with the flow rate.

The results shown in Fig. 12 are summarized in Table 1. Because $\tau = V/Q$, the slope in this case simply corresponds to Q^{-1}. The intercepts of the lines on the vertical axis are generally small compared to the typical estimated time constants (note that, in theory, the lines pass through the origin). The correlation coefficients

Table 1. Summary of the derived time constants with the perfusion phantom

	Flow (L/min)	Slope (s)	Intercept	c.c.	Flow × slope (mL)
τ	0.5	12.75	−3.15	0.959	106.25
	0.7	8.76	−2.22	0.994	102.20
	0.9	7.45	−4.04	0.998	111.75
	1.1	6.02	−4.18	0.981	110.37
MTT	0.5	13.02	−2.24	0.969	108.50
	0.7	8.31	3.07	0.992	96.95
	0.9	7.28	−0.72	0.999	109.20
	1.1	6.26	−2.53	0.984	114.77

between the measurements and the least-squares fitted lines are all higher than 0.95, indicating a good linear relationship between the time constants and the mixing chamber volume. Finally, the product of the volume flow rate and the slope corresponds to the volume of a single dialysis cartridge. The results are shown in the last column, with an average of 107 mL and an SD of 5.7 mL. The average volume is larger than the volume of a single dialysis cartridge (*i.e.,* 79 mL), but close to the total volume when including the extra tubing connecting the injection site, the sample volume and the cartridges (*i.e.,* 114 mL).

DISCUSSION AND CONCLUSIONS

In this study, the time-intensity technique was evaluated and results showed that several factors need to be considered for quantitative flow analysis. For example, the microbubbles were not completely mixed when a large mixing chamber was used. Thus, only relative flow quantification can be achieved and absolute flow quantification is not possible unless the effective mixing volume can be found. In addition, the inflow/outflow directions also affected the derived time constants. Differences between the compartment phantom and the perfusion phantom were also demonstrated. First, the differences in characteristics of the time-intensity may require different signal-processing techniques for the two types of mixing chambers. Second, as shown in Table 1, estimation of the mixing volume was reasonably accurate for the perfusion phantom for a volume up to 351 mL. The MTTs derived from the compartment phantom, on the other hand, were in good agreement with the theory for the 260-mL phantom and became lower than the theory for the 580-mL phantom. By further increasing the total volume, it is possible to explore the relation between the physical volume and the effective volume for the perfusion phantom. Such information is critical in clinical applications of the time-intensity-based quantitative flow analysis techniques.

The derived time constants are related to both the volumetric flow rate Q and the mixing volume V. Hence, the time constant alone is not sufficient for quantitative flow analysis, even if it can be accurately obtained. In other words, the time-intensity technique can only be applied for relative flow analysis if no additional information on the volume or the flow rate is available. For example, one may assume that the mixing chamber volume is fixed and, thus, that the time constant is inversely proportional to the volume flow rate. Alternatively, if the volumetric flow rate can be obtained by other techniques (*e.g.,* conventional Doppler techniques), then the effective volume can be calculated. The derived mixing volume may be directly related to perfusion of a particular organ.

The input function in this paper was approximated by an impulse function. In this case, the output function was used to represent the transfer function of the mixing chamber. This may be invalid in practice because the microbubbles may have traveled through several organs (*i.e.,* mixing chambers) before they reach the region-of-interest (ROI). In this case, the importance of measuring both the input and the output intensities becomes more significant. If both the input and the output can be measured, the transfer function can be obtained by deconvolution (Bates 1991). To measure both the input and the output of the ROI may be practically difficult in clinical situations. In other words, it may be difficult to place both the artery and the vein of an organ in the same image plane. Thus, 3-D imaging may be beneficial in generating the input/output time intensities. As described by Claassen et al. (2001), grey-scale harmonic imaging can be employed for time-intensity measurements. Because the temporal intensities are typically sampled with a rate at about 1 Hz, current nonreal-time 3-D imaging systems may be adequate. Another complication is that many organs have multiple input vessels and multiple output vessels (*e.g.,* liver and brain). Thus, the single input/single output model used in this paper also needs to be modified. Also note that the transfer function obtained by deconvolution is always noisier than the input and output data. Finally, the measured intensity is used to represent concentration in this study. Although such an assumption has been used in previous studies, some studies have also demonstrated the nonlinear relationship between the bubble concentration and the measured intensity (Claassen et al. 2001; Wilson et al. 1993). Thus, the initial concentration of the bolus injection needs to be carefully controlled. Otherwise, the linear system model will not be valid.

More information can be obtained when intensities at both the input and the output are measured. Consider the single-input/single output flow model depicted in Fig. 1; the difference between the number of contrast agents at the input and that at the output at time t is equal to the

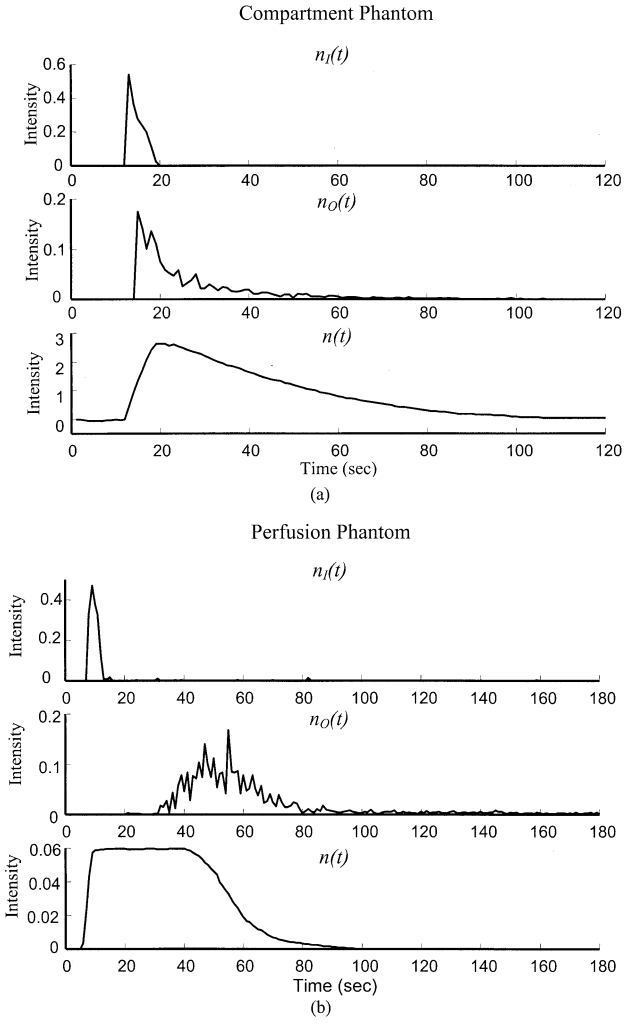

Fig. 13. Input function, $n_I(t)$; output function, $n_o(t)$, and the concentration in the mixing chamber, $n(t)$. (a) Compartment phantom; (b) perfusion phantom.

time derivative of the number of microbubbles in the mixing chamber based on the law of mass conservation. Therefore, we have:

$$V\frac{dn(t)}{dt} = Qn_I(t) - Qn_O(t) = Q(n_I(t) - n_O(t)). \quad (5)$$

By integrating both sides of the above equation, we obtain the following equation:

$$n(t) = \frac{Q}{V}\int_0 (n_I(t) - n_O(t))dt. \quad (6)$$

Equation (6) indicates that, by measuring the concentration at both the input and the output, it is possible to evaluate the concentration in the mixing chamber. Apparently, such a technique is different from the conventional indicator-dilution techniques and has the potential to provide more clinically relevant information. As an example, Fig. 13 shows $n_I(t)$, $n_o(t)$ and $n(t)$ for both a compartment phantom and a perfusion phantom. The three panels in Fig. 13a (from top to bottom) correspond to $n_I(t)$, $n_o(t)$ and $n(t)$, respectively. The three panels in Fig. 13b, on the other hand, are from the perfusion phantom with the same display format as that in Fig. 13a. By deriving proper parameters based on $n(t)$, it may be possible to produce more information for quantitative flow analysis.

Time intensities acquired at the input vessel and the output vessel may also be correlated with the perfusion measurements acquired directly from the mixing chamber. In other words, the hypothesis is that perfusion conditions can be measured outside of the perfused tissue. Particularly for extracranial flow assessment, perfusion in the brain can be assessed by imaging the carotid artery and the jugular vein if such a technique exists. Again, alternative modeling of the problem is required because such a flow system has multiple input vessels and multiple output vessels. Developing new time-intensity-based techniques is the focus of current research.

Acknowledgements—The authord thank Dr. W-C. Yeh for helpful comments on the construction of the mixing chambers. Support supplied by National Science Council under grant NSC 89 to 2213-E-002-128 is also gratefully acknowledged.

REFERENCES

Axel L. Cerebral blood flow determination by rapid-sequence computed tomography: Theoretical analysis. Radiology 1980;137:679–686.

Bates JHT. Deconvolution of tracer and dilution data using the Wiener filter. IEEE Trans Biomed Eng 1991;38:1262–1266.

Blomley MJ, Coulden R, Dawson P, Kormano M, Donlan P, Bufkin C, Lipton J. Liver perfusion studied with ultrafast CT. J Comput Assist Tomogr 1995;19:424–433.

Burns PN, Jaffe CC. Quantitative flow measurements with Doppler ultrasound: Techniques, accuracy and limitations. Radiol Clin North Am 1985;23:641–657.

Chen X, Schwarz K, Phillips D, Steinmetz S, Schlief R. A mathematical model for the assessment of hemodynamic parameters using quantitative contrast echocardiography. IEEE Trans Biomed Eng 1998;45:754–765.

Claassen L, Seidel G, Algermissen C. Quantification of flow rates using harmonic grey-scale imaging and an ultrasonic contrast agent: An *in vitro* and *in vivo* study. Ultrasound Med Biol 2001;27:83–88.

Frinking P, Bouakaz A, Kirkhorn J, Cata F, de Jong N. Ultrasound contrast imaging: Current and new potential methods. Ultrasound Med Biol 2000;26:965–975.

Hindle AJ, Perkins AC. A perfusion phantom for the evaluation of ultrasound contrast agent. Ultrasound Med Biol 1994;20:309–314.

Goldberg B. Contrast agents: Part I. Science and technology. Ultrasound Med Biol 2000;26:S33–S34.

Li P-C, Cheng C-J, Shen C-C. Doppler angle estimation using correlation. IEEE Trans Ultrason Ferroelec Freq Control 2000;47:188–196.

Li P-C, Cheng C-J, Yeh C-K. On velocity estimation using speckle decorrelation. IEEE Trans Ultrason Ferroelec Freq Control 2001; 48(4):1084–1091.

Navin CN, Reinhard S. Advances in echo imaging contrast enhancement. Boston: Kluwer Academic, 1993:43–56.

Ostrander L, Lee B, Silverman D, Groskof R. A compartment model for fluorometric indication of tissue perfusion. IEEE Trans Biomed Eng 1990;37:1017–1023.

Schwarz KQ, Bezante GP, Chen X, Mottley JG, Schlief R. Volumetric arterial flow quantification using echo contrast. An *in vitro* comparison of three ultrasonic intensity methods: Radiofrequency, video and Doppler. Ultrasound Med Biol 1993a;19:447–460.

Schwarz KQ, Bezante GP, Chen X, Schlief R. Quantitative echo contrast concentration measurement by Doppler sonography. Ultrasound Med Biol 1993b;19:289–297.

Schwarz KQ, Chen X, Bezante GP, Phillips D, Schlief R. The Doppler kinetics of microbubble echo contrast. Ultrasound Med Biol 1996; 22:453–462.

Ugolini P, Delouche A, Herment A, Diebold B. *In vitro* flow quantification with contrast agent. Ultrasound Med Biol 2000;26:113–120.

Wilkening W, Helbeck S, Postert T, Federlein J, Rose J, Hoppe P, Buttner T, Ermert H. Brain perfusion imaging using contrast agent specific imaging modes. IEEE Ultrason Sympos 1999;2:1721–1724.

Wilkening W, Postert T, Federlein J, Kono Y, Mattrey R. Ultrasonic assessment of perfusion conditions in the brain and in the liver. IEEE Ultrason Sympos 2000;2:1545–1548.

Wilson B, Shung KK, Hete B, Levene H, Barnhart JL. A feasibility study on quantitating myocardial perfusion with Albunex®, an ultrasonic contrast agent. Ultrasound Med Biol 1993;19:181–191.